



Alteration of the mode of antibacterial action of a defensin by the amino-terminal loop substitution

Bin Gao, Shunyi Zhu *

Group of Animal Innate Immunity, State Key Laboratory of Integrated Management of Pest Insects & Rodents, Institute of Zoology, Chinese Academy of Sciences, 1 Beichen West Road, Chaoyang District, 100101 Beijing, China

ARTICLE INFO

Article history:

Received 25 August 2012

Available online 11 September 2012

Keywords:

Cysteine-stabilized α -helical and β -sheet fold

Insect defensin

Membrane permeability

Micasin

ABSTRACT

Ancient invertebrate-type and classical insect-type defensins (AITDs and CITDs) are two groups of evolutionarily related antimicrobial peptides (AMPs) that adopt a conserved cysteine-stabilized α -helical and β -sheet (CS $\alpha\beta$) fold with a different amino-terminal loop (n-loop) size and diverse modes of antibacterial action. Although they both are identified as inhibitors of cell wall biosynthesis, only CITDs evolved membrane disruptive ability by peptide oligomerization to form pores. To understand how this occurred, we modified micasin, a fungus-derived AITDs with a non-membrane disruptive mechanism, by substituting its n-loop with that of an insect-derived CITDs. After air oxidization, the synthetic hybrid defensin (termed Al-M) was structurally identified by circular dichroism (CD) and functionally evaluated by antibacterial and membrane permeability assays and electronic microscopic observation. Results showed that Al-M folded into a native-like defensin structure, as determined by its CD spectrum that is similar to that of micasin. Al-M was highly efficacious against the Gram-positive bacterium *Bacillus megaterium* with a lethal concentration of 1.76 μ M. As expected, in contrast to micasin, Al-M killed the bacteria through a membrane disruptive mechanism of action. The alteration in modes of action supports a key role of the n-loop extension in assembling functional surface of CITDs for membrane disruption. Our work provides mechanical evidence for evolutionary relationship between AITDs and CITDs.

© 2012 Elsevier Inc. All rights reserved.

1. Introduction

Defensins comprise a structural class of small cationic antimicrobial peptides (AMPs) stabilized by two to five intramolecular disulfide bridges, which have been isolated from almost all cellular organisms [1–5]. Some typical examples include mammalian α -, β - and θ -defensins and invertebrate and plant CS $\alpha\beta$ -type (cysteine-stabilized α -helical and β -sheet) defensins [1,3,4]. In multicellular organisms, these defensins are pivotal effector elements of the innate immune system against microbial infection. Their protective roles have been well documented by *in vivo* targeted disruption of the mosquito *Anopheles gambiae* defensin gene causing the death of the mosquitoes after Gram-positive bacterial infection [6]. Because of high microbicidal potency and structural stability together with low toxicity, these molecules have been considered as ideal templates for developing anti-infective drugs [7,8]. Recently, insect and scorpion venom-derived defensins were also used to construct transgenic *Aedes aegypti* mosquitoes or engineered microbes to block *Plasmodium* transmission [9–11].

Among the CS $\alpha\beta$ -type defensins, ancient invertebrate-type and classical insect-type defensins (AITDs and CITDs) are two groups of

evolutionarily related AMPs (Fig. S1), which have been well studied in terms of their structures, functions and modes of action [1,12–15]. Different from mammalian defensins, these two types of AMPs are principally effective on Gram-positive bacteria. AITDs primarily occur in various species of invertebrates, such as the ancient insect order of Odonata (dragonfly), scorpions, spiders, ticks, and mussels [16,17]. In the tick *Ixodes scapularis*, the AITD gene has undergone extensive expansion to form a large multigene family [18]. By contrast, CITDs were essentially found in phylogenetically recent insect orders (e.g. coleoptera, diptera, hemiptera, hymenoptera, lepidoptera, and phthiraptera) and molluscs [1,19,20], which both belong to the Protostomes. Interestingly, some species belonging to Deuterostomes (e.g. amphioxus) were also found to contain CITDs (data not shown). Recently, it was found that fungal genomes encode AITDs and CITDs [14,16,17]. The structures of AITDs and CITDs include an amino-terminal loop (n-loop) and an α -helical and β -sheet core domain stabilized by two disulfide bridges [12,17]. In spite of overall structural similarity, the length of the n-loop is highly variable between AITDs and CITDs. In comparison with AITDs, CITDs have a longer and conformationally flexible n-loop that is crucial in the involvement of direct interaction with bacterial membrane [12,13]. Although AITDs and CITDs both can bind to the lipid II peptidoglycan precursor to inhibit the cell wall biosynthesis [15,21], only CITDs evolved membrane permeabilization ability [13,22].

* Corresponding author.

E-mail address: Zhusy@ioz.ac.cn (S. Zhu).

Understanding molecular events responsible for the evolution of new modes of action of AMPs helps guide design of new molecules with improved functional features. In this respect, AITDs and CITDs provide an ideal model for such studies. Firstly, the co-existence of the two types of defensins in fungal genomes together with the conservation of their gene structures indicates common origin of AITDs and CITDs in the ancestor of fungi and animals [14,17]. In this case, differential phylogenetic distribution in different animal lineages could be due to lineage-specific defensin

gene loss during evolution; secondly, given that AITDs represent a more primitive form because of their constitutive expression feature [23] and the absence of membrane disruptive ability [15,17,21], we speculate that the evolution of the membrane permeability in CITDs might be a consequence of the n-loop extension in an ancestral AITD scaffold (Fig. 1A).

To test our hypothesis, we generated an engineered defensin by transferring the n-loop of *AIDEF*, a CITD from the harlequin beetle (*Acrocinus longimanus*) [8] to the core region of micasin, a recently

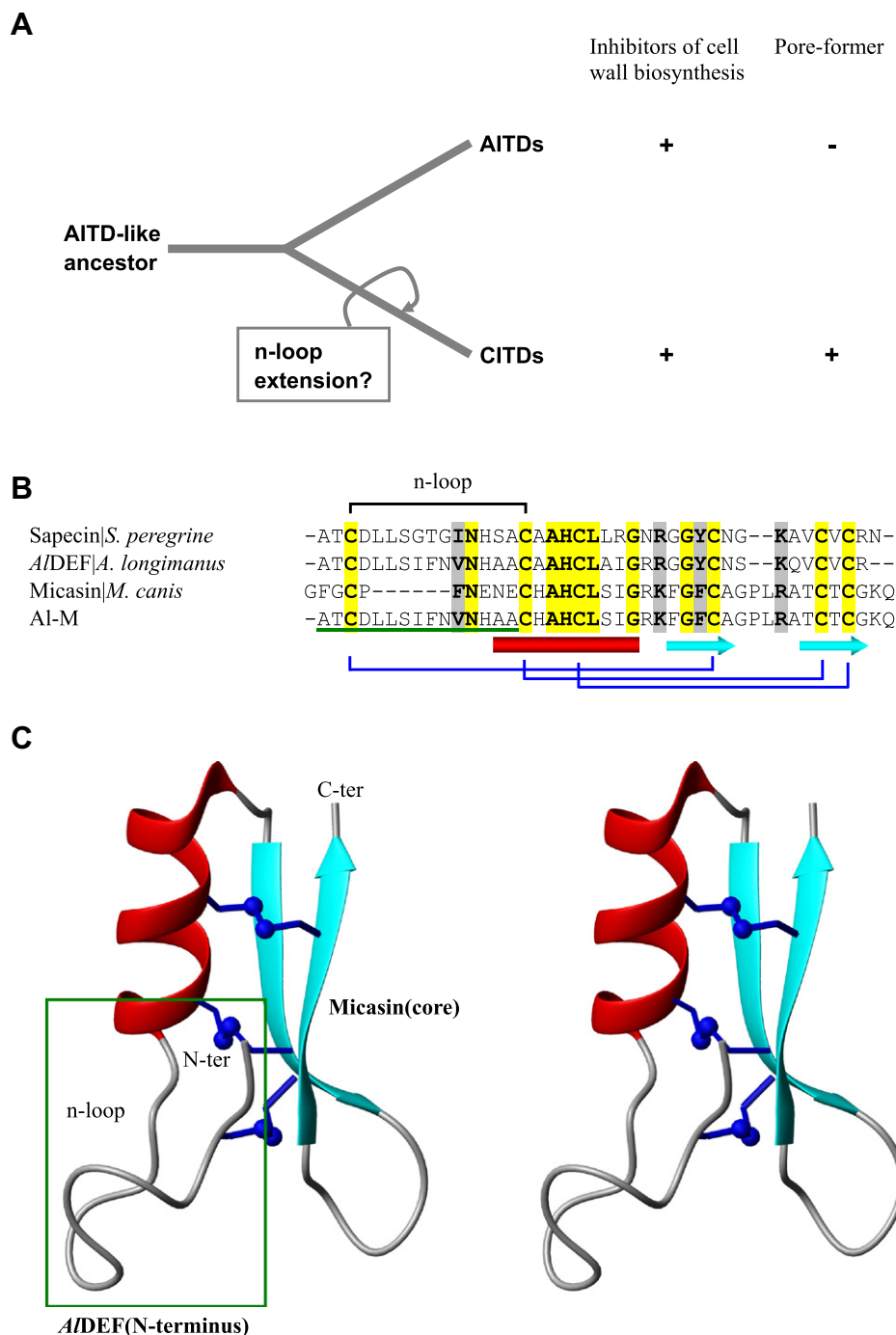


Fig. 1. Molecular design of AI-M based on the proposed evolutionary relationship between AITDs and CITDs. (A) CITDs are presumably evolved from an AITD-like ancestor by the n-loop extension. +, activity; -, no activity. (B) AI-M is a hybrid defensin comprising the n-loop of *AIDEF* underlined in green and the core region of micasin. Identical residues across the alignment are shadowed in yellow and conservative replacements in grey. Secondary structure elements (cylinder, α -helix; arrow, β -strand) and disulfide bridge connectivity patterns are extracted from the model of AI-M and shown at the bottom of the alignment. (C) Stereo view of the ribbon structure of AI-M model. The N-terminus contributed by *AIDEF* is boxed. The model was built by using the experimental coordinates of sapecin (PDB ID: 1L4V) as a template at <http://swissmodel.expasy.org/>. (For interpretation of the references to color in this figure legend, the reader is referred to the web version of this article.)

identified AITD from the dermatophytic fungus *Microsporium canis* with a non-membrane disruptive mode of action [17]. The engineered molecule (herein termed AI-M) obtained membrane permeability to kill *Bacillus megaterium* at low micromolar concentrations. The structural and functional data presented here provide new insights into the evolution of action mode of defensins, in which the key role of n-loop is highlighted.

2. Materials and methods

2.1. Chemical synthesis and oxidative refolding of AI-M

AI-M was chemically synthesized in its reduced form with >95% purity (ChinaPeptides Co., Ltd., Shanghai, China). The peptide was refolded by air oxidization in 0.1 M Tris-HCl buffer (pH 8.0) at 25 °C for 48 h and the reaction products were purified to homogeneity by reversed-phase high-pressure liquid chromatography (rp-HPLC). Purity and molecular mass of the peptide were determined by matrix-assisted laser desorption ionization time-of-flight mass spectrometry (MALDI-TOF MS) on a Kratos PC Axima CFR plus (Shimadzu Co. LTD, Kyoto, Japan).

2.2. Circular dichroism analysis

The circular dichroism (CD) spectrum of AI-M was recorded on a JASCO J-720 spectropolarimeter (Jasco, Tokyo, Japan) at room temperature from 260 to 190 nm by using a quartz cell of 1.0 mm thickness. Data were collected at 0.5 nm intervals with a scan rate of 50 nm/min. CD spectrum measurement was performed by averaging three scans. Data are expressed as mean residue molar ellipticity (θ).

2.3. Antibacterial and membrane permeability assays

The lethal concentration (C_L) of AI-M on *B. megaterium* was determined by the inhibition-zone assay [17], which is a concentration just sufficient to inhibit bacterial growth and thus provides a useful measure to evaluate antibacterial activity of a peptide.

Propidium iodide (PI), a fluorescent dye with highly selective binding to DNA, was used to evaluate membrane permeability of AI-M [17]. In brief, 5×10^5 *B. megaterium* cells in 500 μ l of PBS were mixed with 1 μ M PI for 5 min in the dark. After AI-M was added, the increase in fluorescence, owing to the binding of the dye to intracellular DNA through the destroyed bacterial membrane, was measured using a Hitachi F-4500 fluorescence spectrophotometer (Hitachi High-Technologies, Tokyo). Once the basal fluorescence reaches a constant value, a peptide will be added. Changes in fluorescence arbitrary were monitored ($\lambda_{exc} = 525$ nm; $\lambda_{ems} = 595$ nm) and plotted as arbitrary units.

2.4. Electronic microscopy

For scanning electronic microscopy (SEM), *B. megaterium* cells at exponential growth phase were treated with AI-M at $5 \times C_L$ at 37 °C for 90 min [17]. After centrifugation, bacterial pellets were fixed with 2.5% glutaraldehyde for 1 h, followed by washing three times with PBS. Dehydration was carried out with a series of graded ethanol solution. Cells were then dried using BAL-TEC CPD030 critical point dryer (Germany) before being mounted on carbon tape, sputtered with platinum coating (BAL-TEC SCD005, Germany). Images were visualized in FEI QUANTA 200 (USA). The effects of micasin and meucine-18 on *B. megaterium* cells were also investigated here.

3. Results and discussion

Membrane disruptive and non-membrane disruptive mechanisms represent two basic antibacterial modes of action for AMPs. Studies have shown that binding to lipid II is a common non-membrane disruptive strategy for many defensins (e.g. plectasin, Cg-Defh2, Cg-Defm, Cg-Defh1, and lucifensin) [15,21]. However, among the lipid II-binding peptides some (e.g. CITDs) developed membrane permeability to rapidly kill bacteria [13,15,21,22].

To study the possible role of the long n-loop of CITDs in membrane-disruptive action, we transferred the n-loop of AIDEF (residues Ala¹–Ala¹⁵) to the core domain of micasin (residues Cys¹¹–Gln³⁸), and named the hybrid molecule AI-M (Fig. 1B). Apart from the six conserved cysteines, other 12 non-cysteine residues are also conserved (Asn¹², Ala¹⁸, His¹⁹, Leu²¹, Ile²³, Gly²⁴, Arg²⁵, and Gly²⁸) or conservative replacements (Val¹¹Phe, Arg²⁶Lys, Tyr²⁹Phe, and Lys³³Arg) between AIDEF and micasin (residues numbered according to AIDEF) (Fig. 1B). Because most of the conserved residues are located on the secondary structural elements of the defensins, it is reasonable to infer that AI-M could fold into a

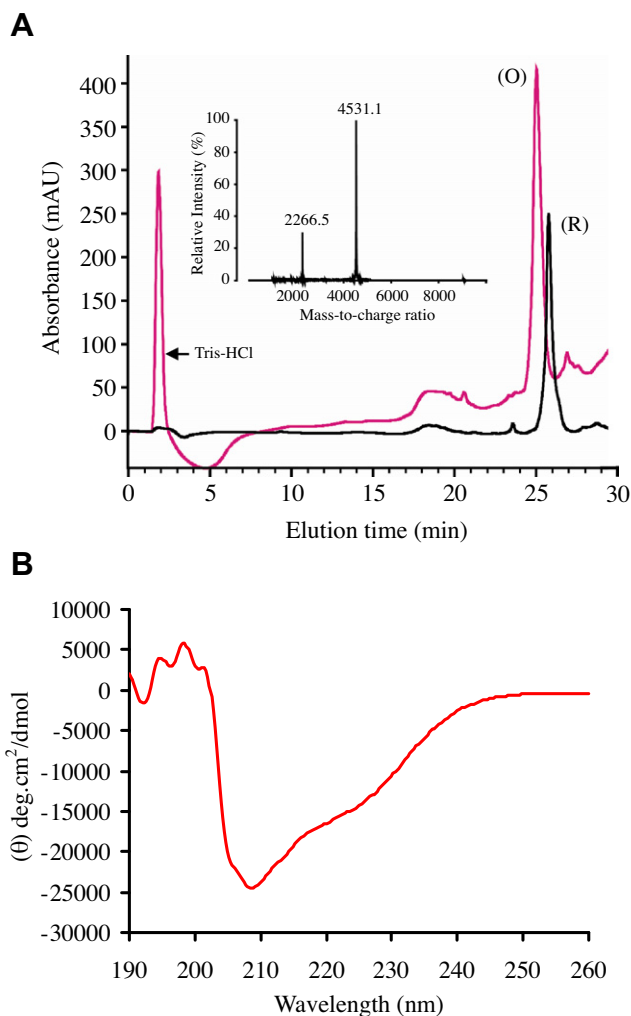


Fig. 2. Oxidative refolding and identification of chemically synthetic AI-M. (A) rp-HPLC showing retention time (T_R) difference between the reduced (R) and oxidized (O) peptides. C_{18} column was equilibrated with 0.1% TFA and purified proteins were eluted from the column with a linear gradient from 0% to 60% acetonitrile in 0.1% TFA within 40 min; Inset, MALDI-TOF MS of the oxidized AI-M. Two main peaks in each spectrum correspond to the singly and doubly protonated forms of the peptide. (B) The CD spectrum of AI-M, measured at a protein concentration of about 0.3 mg/ml dissolved in water.

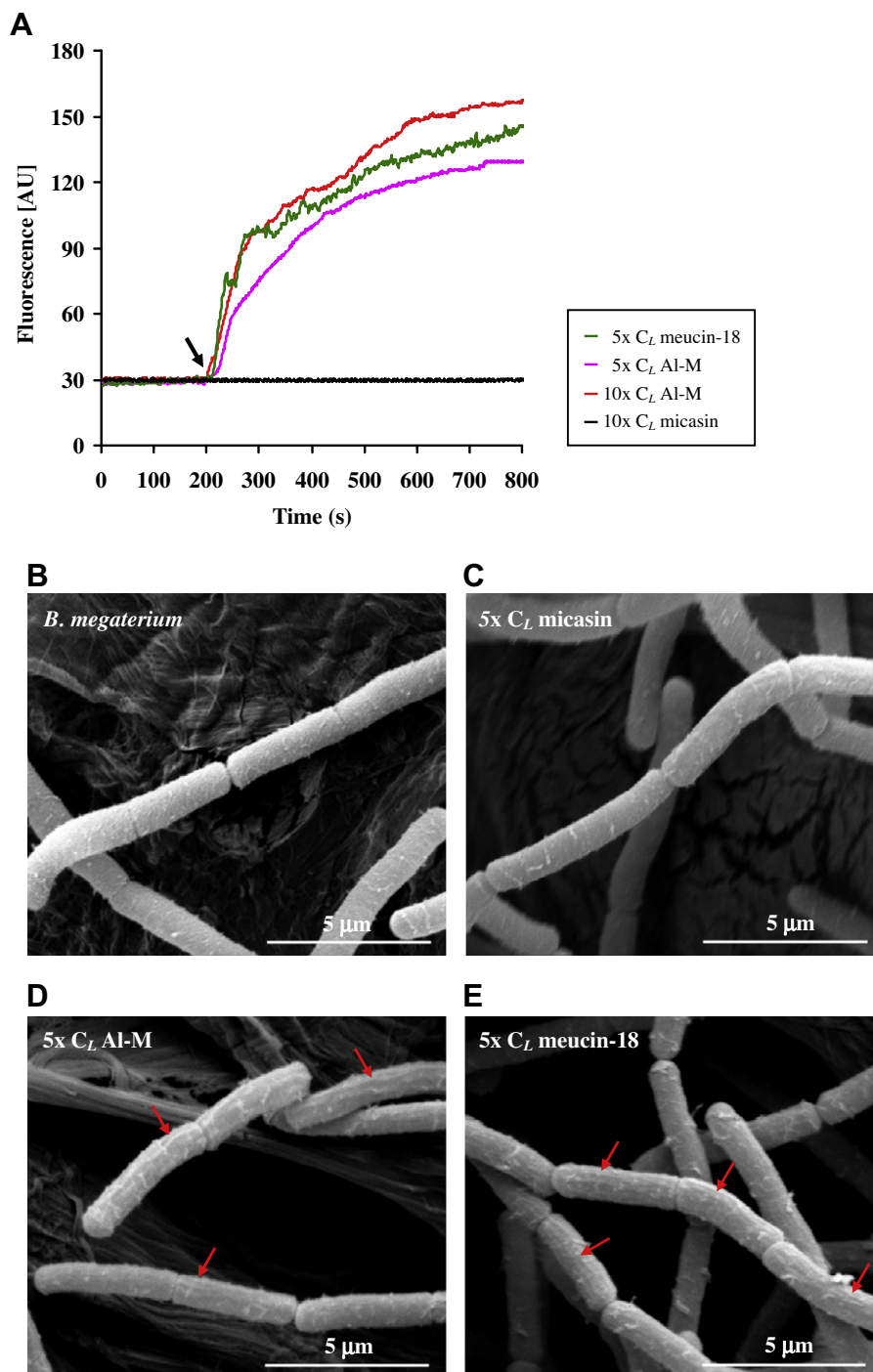


Fig. 3. Effects of AI-M on *B. megaterium* cells. (A) AI-M in contrast to micasin impairs the integrity of *B. megaterium* cellular membranes. In this assay, micasin and meucin-18 were used as negative and positive controls, respectively. (B–E) Scanning electronic microscopic observation of *B. megaterium* cells in the absence or presence of AI-M. The cells were incubated with 5× C_L AI-M at 37 °C for 90 min. Micasin and meucin-18 5× C_L were used as controls. Cells treated by AI-M and meucin-18 show rougher cell surfaces with obvious streak lines, indicated by red arrows. (For interpretation of the references to color in this figure legend, the reader is referred to the web version of this article.)

defensin-like structure, as built by comparative modeling (Fig. 1C). The oxidized AI-M was eluted as a single peak at retention time (T_R) of 25 min, one minute earlier than the reduced peptide (Fig. 2A), in line with more hydrophobic residues buried in a structured molecule. MALDI-TOF MS identified a molecular mass of 4531.10 Da for the peptide, about 6 Da smaller than the theoretical value of 4537.31 Da calculated from its protein sequence, indicating that six hydrogen atoms have been removed to form three

disulfide bridges during oxidative refolding (Fig. 2A). The CD spectrum of AI-M is similar to that of micasin, as identified by a minimum at 208 nm and a maximum around 195 nm (Fig. 2B), experimentally confirming its CS α β -type defensin structure.

AI-M was highly efficacious against *B. megaterium* with a lethal concentration (C_L) of 1.76 μ M. The ability of AI-M to permeabilize the bacterial membrane was assessed with the fluorescent nucleic acid binding dye (PI). Results showed that AI-M destroyed the

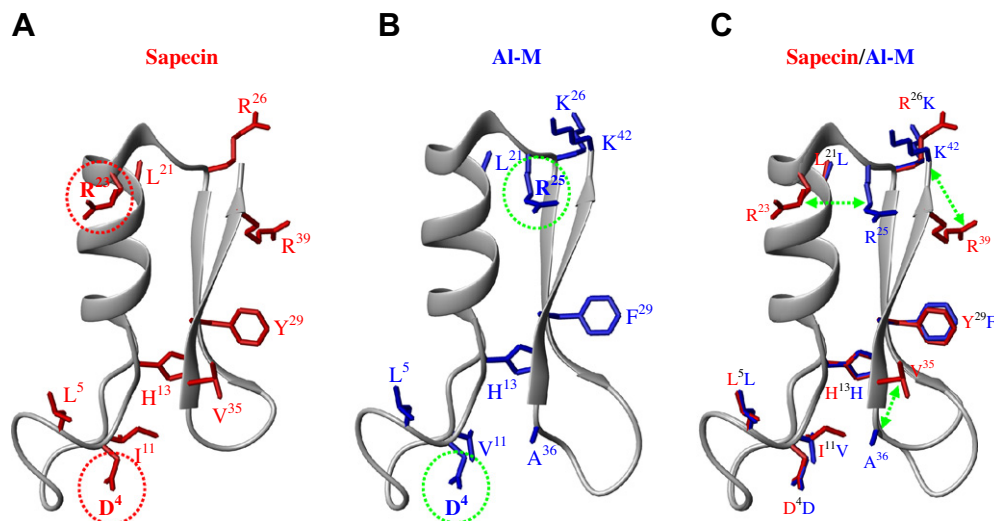


Fig. 4. Analysis of the structural basis for AI-M oligomerization. The ribbon structures of sapecin (A), AI-M (B) and the superimposition between AI-M and sapecin (C). Residues involved in membrane binding and peptide oligomerization are shown as stick models; the complemented residues between AI-M and sapecin are indicated by dotted arrows; and residues putatively involved in peptide oligomerization are indicated by dotted circles.

bacterial membrane integrity, as identified by an immediate fluorescence increase upon exposure of the peptide in a concentration-dependent manner. Meucin-18, a scorpion venom cytolytic peptide [24], exhibited a similar effect to AI-M. No fluorescence increase was observed over 10 min after *B. megaterium* cells were exposed to micasin at $10\times C_L$ (Fig. 3A), consistent with the fact that micasin kills bacteria through a non-membrane disruptive mechanism of action [17]. The membrane damage was further observed by SEM (Fig. 3B–E). As shown in Fig. 3D and E, after the exposure to AI-M or meucin-18 *B. megaterium* cells shriveled up with obvious streak lines in the rough cell surfaces. By contrast, the cells without the peptides or those treated by micasin exhibited a smooth cell surface with normal morphology (Fig. 3B and C).

To date, sapecin is the only one CITD whose molecular basis for channel-forming membrane permeabilization is known, in which eight residues (Leu⁵, Ile¹¹, His¹³, Leu²¹, Arg²⁶, Tyr²⁹, Val³⁵, and Arg³⁹) are identified as key sites involved in the interaction with the membrane and two (Asp⁴ and Arg²³) in oligomerization to form channel pores [13] (Fig. 4A). AI-M displays approximately 50% sequence similarity to sapecin (Fig. 1B). Analysis of its structure allows us to identify a putative functional surface which is similar to that of sapecin. As shown in Fig. 4B and C, of the ten functional residues of sapecin, seven were found to have structurally equivalent residues in AI-M, including four residues (Asp⁴, Leu⁵, Val¹¹ and His¹³) provided by the n-loop of AIDEF and three residues (Leu²¹, Lys²⁶, and Phe²⁹) contributed by the core region of micasin. In addition, no residues in AI-M perfectly match Arg²³, Val³⁵, and Arg³⁹ of sapecin but they could be complemented by Arg²⁵, Ala³⁶, and Arg⁴² in AI-M due to the adjacent position of these residues in the structures (Fig. 4C). These analyses identified Asp⁴ and Arg²⁵ as putative residues implicated in AI-M oligomerization by electrostatic interaction (Fig. 4B). In fact, many native CITDs that lack a basic residue at position 23 instead have a basic residue at position 25 [13]. The observation that the core region of micasin contains six putative functional residues for the membrane permeability of AI-M supports the evolutionary intermediate position of micasin between AITDs and CITDs.

Taken together, our work for the first time sheds light on the functional evolution of CS α -type defensins, in which the membrane permeability of CITDs might be developed through the extension of the n-loop in an ancestral AITD scaffold that has pre-evolved several key sites to assemble a complete functional surface.

Acknowledgments

This work was supported by the National Basic Research Program of China (2010CB945300) and the National Natural Science Foundation of China (30730015 and 30921006).

Appendix A. Supplementary data

Supplementary data associated with this article can be found, in the online version, at <http://dx.doi.org/10.1016/j.bbrc.2012.08.143>.

References

- [1] J.-L. Dimarcq, P. Bulet, C. Hetru, J. Hoffmann, Cysteine-rich antimicrobial peptides in invertebrates, *Biopolymers* 47 (1998) 465–477.
- [2] S. Zhu, Evidence for myxobacterial origin of eukaryotic defensins, *Immunogenetics* 59 (2007) 949–954.
- [3] E. Arnett, S. Seveau, The multifaceted activities of mammalian defensins, *Curr. Pharm. Des.* 17 (2011) 4254–4269.
- [4] O. Carvalho Ade, V.M. Gomes, Plant defensins and defensin-like peptides – biological activities and biotechnological applications, *Curr. Pharm. Des.* 17 (2011) 4270–4293.
- [5] R.I. Lehrer, W. Lu, α -Defensins in human innate immunity, *Immunol. Rev.* 245 (2012) 84–112.
- [6] S. Blandin, L.F. Moita, T. Köcher, M. Wilm, F.C. Kafatos, E.A. Levashina, Reverse genetics in the mosquito *Anopheles gambiae*: targeted disruption of the defensin gene, *EMBO Rep.* 3 (2002) 852–856.
- [7] K. Thevissen, H.-H. Kristensen, B.P. Thomma, B.P. Cammue, I.E. Francois, Therapeutic potential of antifungal plant and insect defensins, *Drug Discov. Today* 12 (2007) 966–971.
- [8] C. Landon, F. Barbault, M. Legrain, M. Guenneugues, Rational design of peptides active against the gram positive bacteria *Staphylococcus aureus*, *Proteins* 72 (2008) 229–239.
- [9] V. Kokoza, A. Ahmed, S. Woon Shin, N. Okafor, Z. Zou, A.S. Raikhel, Blocking of *Plasmodium* transmission by cooperative action of cecropin A and defensin A in transgenic *Aedes aegypti* mosquitoes, *Proc. Natl. Acad. Sci. USA* 107 (2010) 8111–8116.
- [10] W. Fang, J. Vega-Rodríguez, A.K. Ghosh, M. Jacobs-Lorena, A. Kang, R.J. St Leger, Development of transgenic fungi that kill human malaria parasites in mosquitoes, *Science* 331 (2011) 1074–1077.
- [11] S. Wang, A.K. Ghosh, N. Bongio, K.A. Stebbings, D.J. Lampe, M. Jacobs-Lorena, Fighting malaria with engineered symbiotic bacteria from vector mosquitoes, *Proc. Natl. Acad. Sci. USA* 109 (2012) 12734–12739.
- [12] B. Cornet, J.-M. Bonmatin, C. Hetru, J.A. Hoffmann, M. Ptak, F. Vovelle, Refined three-dimensional solution structure of insect defensin A, *Structure* 3 (1995) 435–448.
- [13] K. Takeuchi, H. Takahashi, M. Sugai, H. Iwai, T. Kohno, K. Sekimizu, S. Natori, I. Shimada, Channel-forming membrane permeabilization by an antibacterial protein, sapecin: determination of membrane-buried and oligomerization surfaces by NMR, *J. Biol. Chem.* 279 (2004) 4981–4987.

- [14] S. Zhu, Discovery of six families of fungal defensin-like peptides provides insights into origin and evolution of the CS α β defensins, *Mol. Immunol.* 45 (2008) 828–838.
- [15] T. Schneider, T. Kruse, R. Wimmer, I. Wiedemann, V. Sass, U. Pag, A. Jansen, A.K. Nielsen, P.H. Mygind, D.S. Raventós, S. Neve, B. Ravn, A.M. Bonvin, L. De Maria, A.S. Andersen, L.K. Gammelgaard, H.G. Sahl, H.H. Kristensen, Plectasin, a fungal defensin, targets the bacterial cell wall precursor Lipid II, *Science* 328 (2010) 1168–1172.
- [16] P.H. Mygind, R.L. Fischer, K.M. Schnorr, M.T. Hansen, C.P. Sönksen, S. Ludvigsen, D. Raventós, S. Buskov, B. Christensen, L. De Maria, O. Taboureau, D. Yaver, S.G. Elvig-Jørgensen, M.V. Sørensen, B.E. Christensen, S. Kjaerulff, N. Frimodt-Møller, R.I. Lehrer, M. Zasloff, H.H. Kristensen, Plectasin is a peptide antibiotic with therapeutic potential from a saprophytic fungus, *Nature* 437 (2005) 975–980.
- [17] S. Zhu, B. Gao, P.J. Harvey, D.J. Craik, Dermatophytic defensin with anti-infective potential, *Proc. Natl. Acad. Sci. USA* 109 (2012) 8495–8500.
- [18] Y. Wang, S. Zhu, The defensin gene family expansion in the tick *Ixodes scapularis*, *Dev. Comp. Immunol.* 35 (2011) 1128–1134.
- [19] B. Gao, S. Zhu, Identification and characterization of the parasitic wasp *Nasonia* defensins: positive selection targeting the functional region?, *Dev. Comp. Immunol.* 34 (2010) 659–668.
- [20] W. Xu, M. Faisal, Defensin of the zebra mussel (*Dreissena polymorpha*): molecular structure, *in vitro* expression, antimicrobial activity, and potential functions, *Mol. Immunol.* 47 (2010) 2138–2147.
- [21] P. Schmitt, M. Wilmes, M. Pugniere, A. Aumelas, E. Bachere, H.-G. Sahl, T. Schneider, D. Destoumieux-Garzon, Insight into invertebrate defensin mechanism of action, *J. Biol. Chem.* 285 (2010) 29208–29216.
- [22] S. Cociancich, A. Ghazi, C. Hetru, J.A. Hoffmann, L. Letellier, Insect defensin, an inducible antibacterial peptide, forms voltage-dependent channels in *Micrococcus luteus*, *J. Biol. Chem.* 268 (1993) 19239–19245.
- [23] M. Charlet, S. Chernysh, H. Philippe, C. Hetru, J.A. Hoffmann, P. Bulet, Isolation of several cysteine-rich antimicrobial peptides from the blood of a mollusc, *Mytilus edulis*, *J. Biol. Chem.* 271 (1996) 21808–21813.
- [24] B. Gao, P. Sherman, L. Luo, J. Bowie, S. Zhu, Structural and functional characterization of two genetically related meucins highlights evolutionary divergence and convergence in antimicrobial peptides, *FASEB J.* 23 (2009) 1230–1245.